Supernova Cosmology in the Big Data Era

108

Richard Kessler

Abstract

Here we describe large "Big Data" Supernova (SN) Ia surveys, past and present, used to make precision measurements of cosmological parameters that describe the expansion history of the universe. In particular, we focus on surveys designed to measure the dark energy equation of state parameter w and its dependence on cosmic time. These large surveys have at least four photometric bands, and they use a rolling search strategy in which the same instrument is used for both discovery and photometric follow-up observations. These surveys include the Supernova Legacy Survey (SNLS), Sloan Digital Sky Survey II (SDSS-II), Pan-STARRS 1 (PS1), Dark Energy Survey (DES), and Large Synoptic Survey Telescope (LSST). We discuss the development of how systematic uncertainties are evaluated, and how methods to reduce them play a major role is designing new surveys. The key systematic effects that we discuss are (1) calibration, measuring the telescope efficiency in each filter band, (2) biases from a magnitude-limited survey and from the analysis, and (3) photometric SN classification for current surveys that don't have enough resources to spectroscopically confirm each SN candidate.

Contents

R. Kessler (✉)
Department of Astronomy and Astrophysics, Kavli Institute for Cosmological Physics, University of Chicago, Chicago, IL, USA
e-mail: kessler@kicp.uchicago.edu

A.W. Alsabti, P. Murdin (eds.), *Handbook of Supernovae*,
https://doi.org/10.1007/978-3-319-21846-5_107

1 Introduction

As described in previous sections of this handbook, observations of a few dozen type Ia supernovae (SNe Ia) were used to discover cosmic acceleration (Perlmutter et al. 1999; Riess et al. 1998). After standardizing the rest-frame supernova (SN) brightness to within about 15 %, corresponding to 7 % precision in distance, the observed brightness of distant SNe Ia at redshift $z \approx 0.5$ ($\sim$5 billion light years away) was compared to nearby SNe Ia at redshift $z < 0.1$. The key finding was that the distant SNe Ia are $\sim$30 % fainter than expected from a model of the universe containing only matter and undergoing gravitational contraction. The unexpected faintness led to the conclusion that cosmic acceleration has pushed these distant SNe Ia further away, contrary to the long-held conventional wisdom of cosmic deceleration.

In the early years of studying type Ia supernovae (SNe Ia), observing and spectroscopically confirming each SN Ia required serious effort to coordinate resources with multiple instruments. Given the rarity and difficulty in acquiring these gems, many of the early pioneers knew their SNe Ia by name and could rattle off detailed information about the SN properties just like they could describe their own child. It is still quite common to hear astronomers describing newly discovered SNe Ia with comparisons such as "this one is 1991T-like" or "2002cx-like." As samples become larger, the individuality of each SNe Ia becomes less important, and instead we focus more on their bulk properties.

In spite of the name of this section title, "Big Data" is not a standard term used by astronomers studying SNe Ia. I will therefore arbitrarily define surveys in the Big Data era as having the following features:

1. they work in "rolling-search" mode, meaning that the same telescope is used for both discovery and following each light curve through broadband filters.
2. SN Ia light curves are measured in at least three broadband filters, giving two-color measurements.
3. The transient search is associated with a wide-area survey using the same instrument.

The advantage of feature (1) is that the earliest light curve points are observed with the same high-quality instrument, and one can recover early and late epochs where the SN is too faint to pass the detection threshold. Other advantages of using a single instrument are to simplify the calibration and to predict the effect of selection

biases that favor brighter objects. The advantage of (2) is that since correcting the SN brightness for color is the main source of astrophysical uncertainty, having two nearly independent color measurements allows for important systematic checks. The advantage of (3) is that the associated wide-area survey typically results in more effort and resources for calibration, which is currently the largest source of systematic uncertainty.

Ironically, the amount of data is not listed as a criteria for Big Data. Instead, the three definitions are related to data quality. In short, to improve measurements of cosmological parameters with SNe Ia, it is the improving data quality that drives larger data samples.

Other notable aspects of Big Data include multiyear observing campaigns that require a dedicated team with a long-term commitment, large-scale computing platforms to process hundreds of Gb of new data in less than a day in order to find targets for spectroscopic follow-up observations, and extensive monitoring with fake SNe Ia overlaid near galaxies on real images.

An outline of this article is as follows. A brief overview of light curve fitting and the SN Ia Hubble diagram is given in Sect. 2. Past Big Data surveys are reviewed in Sect. 3, and current and future surveys are described in Sect. 4. The main systematic uncertainties are discussed in Sect. 5, including calibration, selection biases, and photometric classification.

2 Overview of Fitting Light Curves and Hubble Diagrams

The Big Data discussions rely on the concept of light curve fitting (LC fitting) and Hubble diagram (HD), so here we give a brief overview of these concepts. The main goal of an LC fit is to determine the SN Ia color, stretch, and brightness; the color and stretch parameters are then used to standardize the brightness to within 15 %, and this 15 % irreducible scatter is from intrinsic brightness variations that do not correlate with other observables. The stretch is the relative light curve width compared to the average width of all SNe Ia, and the color parameter is roughly the $B - V$ color at peak brightness. The wavelength dependence of SN Ia luminosities, known as a color law, is used to determine the color parameter. Typical light curve fits are shown in Fig. 1 for SDSS-II. Since observed SN light has been redshifted, the measured broadband magnitudes are combined with an average SN Ia spectrum to compute rest-frame magnitudes. The conversion factor between an observer-frame and rest-frame magnitude is referred to as K-correction (Nugent et al. 2002).

To standardize the SN Ia magnitude, a linear function of the stretch and color works well. Quadratic terms have been tried, but not convincingly found. The linear coefficients for stretch and color, along with the color law, are determined from a process known as "training." The training sample usually contains the highest quality light curves and those with good-quality spectra. For some of the early SN cosmology results (before Big Data), the color law was often assumed to be the same as that for the Milky Way (Galactic reddening law). Training with the `SALT-II`

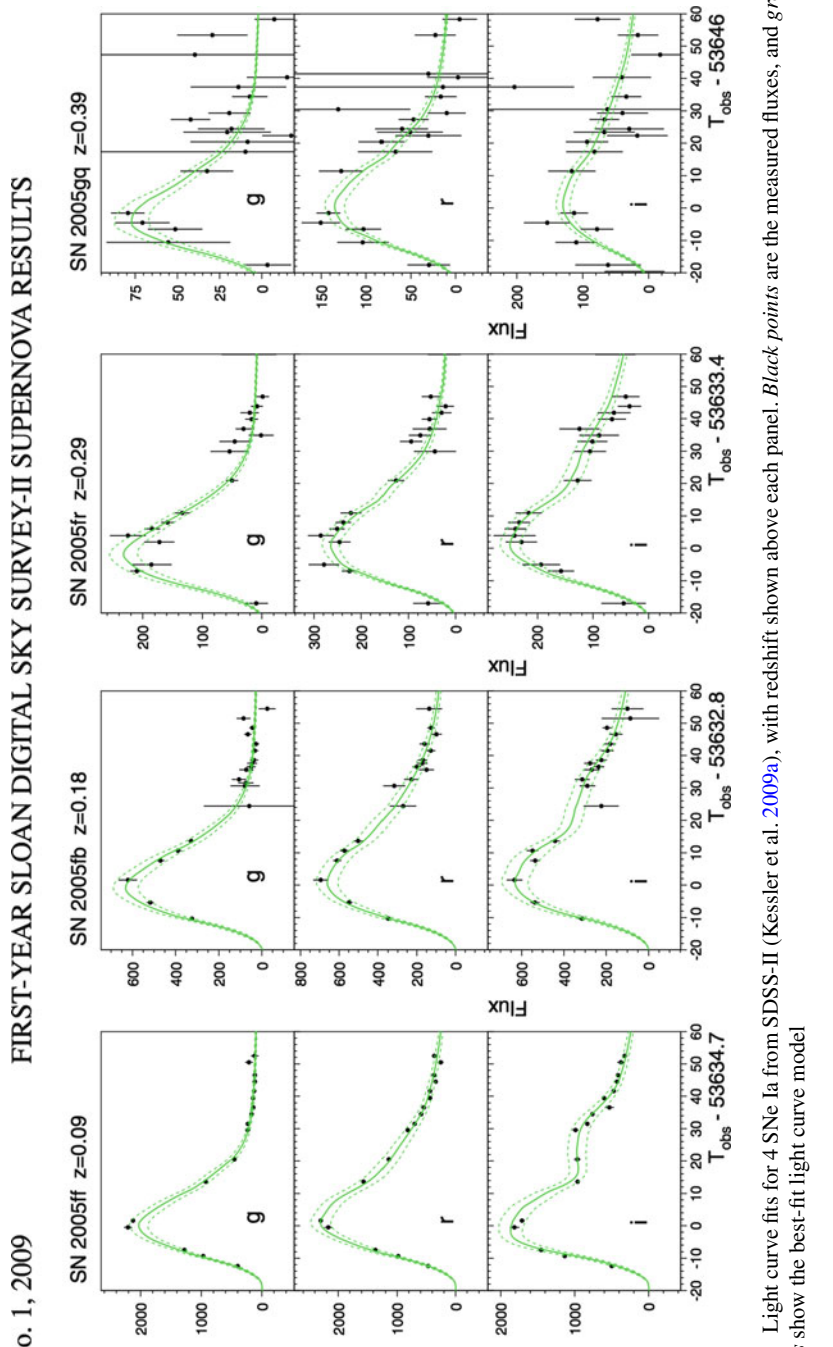

Fig. 1 Light curve fits for 4 SNe Ia from SDSS-II (Kessler et al. 2009a), with redshift shown above each panel. *Black points* are the measured fluxes, and *green curves* show the best-fit light curve model

method (Guy et al. 2010) on larger samples, however, showed that the empirically determined color law is quite different in the ultraviolet (UV) region, which has a significant effect on higher-redshift SNe.

The determination of cosmological parameters comes from fitting a SN Ia Hubble diagram (HD), which is a plot of distance modulus (μ, defined below) versus redshift. Consider an ideal situation of measuring bolometric mags ($m_{\rm obs}$) with 100 % efficiency and no Galactic extinction, and each SN Ia rest-frame mag ($M_{\rm rest}$) is fixed to a constant value: in this scenario the distance modulus is given by $\mu = m_{\rm obs} - M_{\rm rest}$, the difference between the observed mag through a telescope and the rest-frame mag that would be observed at a distance of 10 kpc. In a universe with no expansion, no curvature, and a SN at distance D from Earth, μ is simply related to the inverse-square law,

$$\mu = -2.5\log[(10{\rm pc}/D)^2] = 5\log(D/10{\rm pc}). \tag{1}$$

Note that $\mu = 0$ at 10 pc, and it is defined to increase with distance. In an expanding universe, the distance D is replaced with the *luminosity distance*, $D_{\mathscr{L}}$, which depends on the redshift (z) and cosmological parameters ($\overrightarrow{\mathbf{C}}$),

$$D_{\mathscr{L}} = c(1+z)\int dz/H(z,\overrightarrow{\mathbf{C}}), \quad \mu = 5\log(D_{\mathscr{L}}/10{\rm pc}). \tag{2}$$

$H(z,\overrightarrow{\mathbf{C}})$ is the Hubble parameter as a function of redshift, $\overrightarrow{\mathbf{C}}$ is an arbitrary set of fundamental parameters that describe cosmic expansion, and c is the speed of light. The Hubble parameter is most commonly expressed as

$$H(z,\overrightarrow{\mathbf{C}}) = H(z,\Omega_{\rm M},\Omega_\Lambda,w) = H_0\left[\Omega_\Lambda^0(1+z)^{3(1+w)} + \Omega_{\rm M}^0(1+z)^3\right]^{1/2} \tag{3}$$

where $\Omega_{\rm M}^0, \Omega_\Lambda^0$ are today's energy density of dark matter and dark energy, respectively, and w is the dark energy equation of state parameter. Note that $w = -1$ corresponds to a cosmological constant because $\Omega_\Lambda(z, w = -1) = \Omega_\Lambda^0$ never changes. The radiation density today is $\Omega_\gamma \sim 10^{-5}$ and is small enough to be ignored in SN analyses.

To summarize, measurements of redshift (z) and distance modulus (μ) for each SN Ia are used to construct an HD, and the HD is fit to Eqs. 2 and 3 in order to determine $\Omega_{\rm M}$, Ω_Λ, and w. A flatness prior is often used in which there is no curvature and thus $\Omega_{\rm M} + \Omega_\Lambda = 1$; this prior is based on measurements of the cosmic microwave background.

Measuring an accurate redshift from spectroscopic features is relatively straightforward with adequate signal to noise, but measuring a distance with $\mu = m_{\rm obs} - M_{\rm rest}$ is overly simplistic because (1) the telescope efficiency depends on observed wavelength, (2) emitted light is redshifted when reaching Earth, (3) SN light reddens as it passes through dust in the host galaxy, (4) SN light reddens as it passes through Milky Way dust, (5) SN mag changes with time, and (6) $M_{\rm rest}$ varies with each SN Ia

and requires an empirical correction based on color and stretch. A full description of determining μ is beyond the scope of this section, but for the discussion that follows, we assume that the above effects have been accounted for.

3 Big Data Surveys: Past

We begin with the Supernova Legacy Survey (Astier et al. 2006, SNLS) that collected data from 2003 to 2008 using the 3.5 m Canada-France-Hawaii Telescope (CFHT). SNLS covered four 1-deg^2 patches and was designed to measure accurate light curves for high redshift SNe Ia, $0.3 \leq z \leq 1$. They used four broadband filters, denoted $griz$, with central wavelengths 4900, 6300, 7690, and 8840 Å, respectively. At their lowest redshift ($z = 0.3$), the g band central wavelength maps to ∼3800 Å in the rest frame, which is well within the range of SN Ia light curve models. At their highest redshift ($z = 1$), the g band corresponds to ∼2500 Å in the rest frame, which is too far in the ultraviolet (UV) to be useful for light curve fitting; in practice the g-band is useful up to redshifts $z \leq 0.6$. The remaining three bands (riz) are useful for light curve fitting over the entire redshift range, thus satisfying the two-color requirement. While there are two colors available over the entire redshift range, note that at $z = 1$, the rest-frame wavelength range is compressed to 3150–4420 Å, which covers only the bluest region of the 3000–7000 Å wavelength range spanned by the `SALT-II` model (Guy et al. 2010). This limited wavelength coverage at higher redshifts results in larger uncertainties on the fitted parameters.

Shortly after SNLS began, the Sloan Digital Sky Survey II (SDSS-II) used the 2.5 m telescope at the Apache Point Observatory to repeatedly search 300 deg^2 in the fall seasons of 2005–2007. They discovered and measured light curves for SNe Ia in the redshift range $z < 0.4$ (Frieman et al. 2008) using five broadband filters ($ugriz$), although the sensitivity in the u and z bands was far less than in the gri bands. To monitor efficiencies from software selection and human scanners, this is the first Big Data survey that injected fake SNe Ia onto images during the survey in order to provide immediate feedback on the performance of discovering new SNe.

Both SDSS-II and SNLS discovered and spectroscopically confirmed about 500 SNe Ia. Each team combined a subset of their SN sample with SN samples in the literature and with SDSS results on baryon acoustic oscillations (Eisenstein et al. 2005). They independently published their own cosmology results measuring $\Omega_{\rm M}$ and the dark energy equation of state parameter w and found w consistent with -1 to within about 10 % (Astier et al. 2006; Conley et al. 2011; Kessler et al. 2009a). These results included a detailed treatment of systematic uncertainties. Two noteworthy advances are calibration and bias corrections from simulations. The calibration is needed to accurately compare fluxes measured in different passbands within SDSS-II, SNLS, and the other survey instruments providing lower-redshift SNe Ia (see Sect. 5.1 below). While both teams worked for years to reach ∼1 % precision on their calibration, their results were nonetheless systematics limited by calibration.

The second major improvement in these measurements is the use of detailed Monte Carlo simulations to measure and correct for biases (see Sect. 5.2 below). The largest effect is the well-known Malmquist bias in which intrinsically brighter objects are selected at higher redshift, resulting in a redshift-dependent bias in the Hubble diagram. Subtle fitting biases may also be present. The SNLS approach was to fully analyze images with roughly a million fake SNe Ia overlaid near galaxies (Perrett et al. 2010). The SDSS approach was to use a much smaller number of fakes to characterize the software detection efficiency vs. signal to noise and to analytically characterize the instrumental performance (Kessler et al. 2009b). The SNLS simulation has the advantage of being a more faithful representation of real data at the cost of requiring large amounts of computing. The SDSS approach has the advantage of speed, allowing for many iterations with different SN models and assumptions, and it can be used on arbitrary surveys without acquiring their images.

Both teams realized that their cosmology results were systematics limited and that adding more data would be of little use without making fundamental improvements to the analysis. These two teams joined forces in 2010, and in a joint analysis, they produced a Hubble diagram with 740 SNe Ia (Fig. 2) and reduced the w-uncertainty to 6 % (Betoule et al. 2014). Their first major improvement was to compare stellar magnitudes in fields observed by both SDSS-II, SNLS, and the

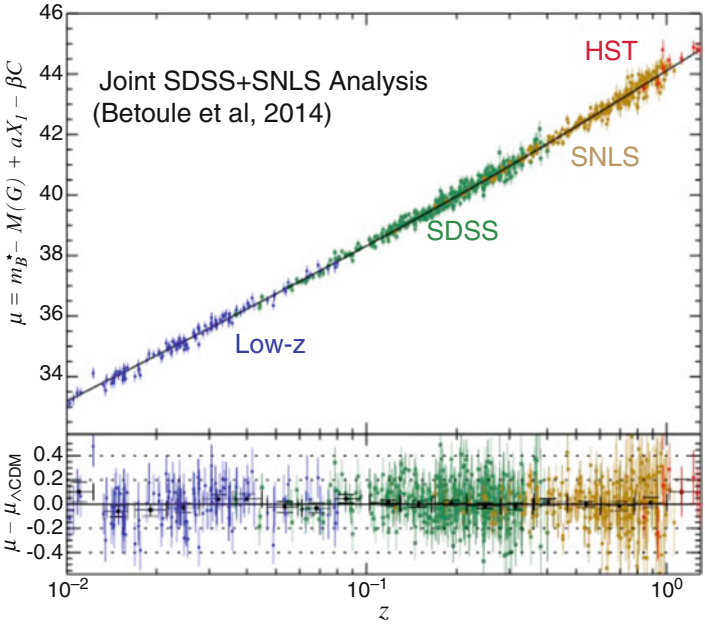

Fig. 2 *Top panel* shows the Hubble diagram from the joint SDSS + SNLS analysis (Betoule et al. 2014), with each data subset labeled. *Bottom panel* shows the distance residuals, $\mu - \mu_{\Lambda CDM}$, where μ is the measured distance and $\mu_{\Lambda CDM}$ is the calculated distance from the best-fit ΛCDM model. ΛCDM refers to a flat ($\Omega_M + \Omega_\Lambda = 1$) universe with $w = -1$

Hubble Space Telescope (HST), where the stars measured with HST are used as the standard reference for all SN magnitude measurements (Sect. 5.1). This effort led to reducing the calibration uncertainty by about a factor of 2 (Betoule et al. 2013), which reduces the overall w-uncertainty by $\sim$20 %.

The second major improvement was to use simulations to rigorously evaluate systematic uncertainties from the 15 % irreducible (intrinsic) Hubble scatter and from the so-called "training" process that determines the parameters used to standardize the SN Ia luminosity as a function of its stretch and color. Cosmology fitting programs have always added the intrinsic scatter ($\sigma_{\rm int}$) in quadrature with the measured uncertainties, and this is equivalent to assuming that the intrinsic scatter for a given SN Ia is characterized by a single number at all wavelengths and epochs. It is unlikely that the SN Ia brightness varies in such a simple manner, and thus the joint analysis team analyzed simulations with several different intrinsic scatter models that include significant wavelength variations. The other systematic effect, SN Ia training, is a very complex process for which previous training uncertainties were either ignored or based on educated guesses. Using the `SALT-II` light curve model, Mosher et al. (2014) used detailed simulations to evaluate the combined effect of training, light curve fitting, and using $\sigma_{\rm int}$ in the cosmology fitting. They found a w-uncertainty of $\sim$0.02, well below the current constraints, but these effects could become important in future surveys with reduced uncertainties.

The most recent Big Data survey to finish is Pan-STARRS 1 (Kaiser et al. 2002, PS1), which repeatedly observed 70 deg^2 with a 1.8 m telescope in Hawaii. As with previous results, their first cosmology result was based on spectroscopically confirmed SNe Ia, and the precision was limited by calibration uncertainties. An interesting contribution of PS1 is their 3π sky calibration for which bright stars (mag $<$ 21) in 3/4 of the sky are calibrated to within 0.005 mag (Schlafly et al. 2012). Scolnic et al. (2015) used this 3π calibration to propose a new "Supercal" method for SN Ia samples that overlap PS1. Instead of comparing tertiary stars (near each SN Ia) to HST spectrophotometric standards, they compare to stars measured by PS1. While the HST calibration may have a larger uncertainty, the relative uncertainty among the SN Ia samples can in principle be reduced to the 0.005 mag level after applying calibration offsets to correct for discrepancies. Scolnic et al. (2015) compared PS1 against star catalogs from SDSS, SNLS, CSP, and numerous low-z samples; most of the offsets are consistent with the reported 0.01 mag uncertainties, but discrepancies up to 0.03 mag were found. Applying these mag offsets to each non-PS1 sample, the equation of state parameter w changes by nearly 0.03 or half the current uncertainty.

4 Present and Future Big Data Surveys: DES and LSST

The Dark Energy Survey (DES) began a 5-year program in 2013 that includes a deep transient search over ten fields covering 30 deg^2. This survey uses the 4 m Blanco telescope at CTIO with a new 500 megapixel camera (Flaugher et al. 2015) featuring

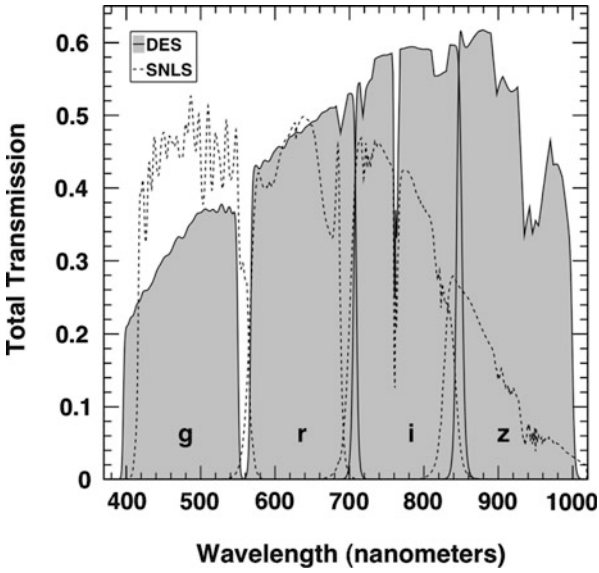

Fig. 3 Total transmission for DES filters and telescope (*shaded*) compared with transmissions from SNLS (*dashed*), a previous generation survey

a 3 deg^2 field of view and 62 CCDs with enhanced sensitivity in the near infrared as shown in Fig. 3. The improved sensitivity in the i and z bands should result in finding more SNe at higher redshifts. Compared to a similar predecessor, SNLS, the DES-SN search covers $\times 7$ more area and has significantly better sensitivity in the z band. However, with limited spectroscopic resources, it is expected that the size of the spectroscopically confirmed subset in DES-SN will be similar to that in SNLS ($\sim$400). To take advantage of the increased SN statistics, DES-SN will rely on photometric classification for the majority of SNe Ia (see Sect. 5.3 for more details). Although DES-SN will spectroscopically confirm only a small subset of SNe Ia, there are large multi-fiber spectroscopic programs to measure accurate host-galaxy redshifts for most of the SNe.

To improve calibration, DES has two new systems in its arsenal. First, the telescope transmission versus wavelength, denoted $\mathrm{T}(\lambda)$, and out-of-band leakage are measured with a "DECal" system in which an artificial source of monochromatic light is sent into the telescope. Around the telescope entrance, there are NIST-calibrated photodiodes whose efficiency vs. wavelength is well known. The ratio of CCD signal to photodiode signal is a measure of the combined transmission of the telescope mirror, filters, and CCDs. Note that the definition of magnitude is sensitive to the shape of $\mathrm{T}(\lambda)$ and not the absolute transmission, and therefore there is no need to track the flux ratio of light entering the telescope and photodiodes. In other words, the photodiodes can be placed at an arbitrary distance from the light source as long as the DECal equipment does not move during a measurement of $\mathrm{T}(\lambda)$.

$\mathrm{T}(\lambda)$ is typically measured with a 2 nm bandpass and in 2 nm steps and covers the $griz$ wavelength range $300 < \lambda < 1100$ nm. Naively such measurements would take place during daytime, but due to light leaks in the dome, the $\mathrm{T}(\lambda)$ measurements

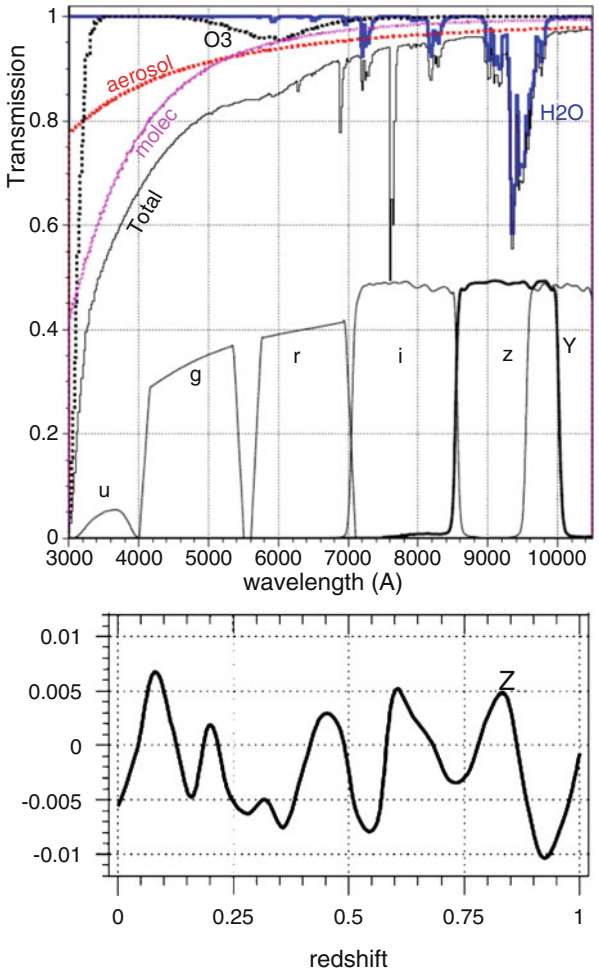

Fig. 4 *Left panel* shows components of the atmosphere transmission at CTIO, along with approximate DES filter transmission curves. Note that the H_2O component (water vapor) overlaps the z band. For a 10 mm change in PWV that is not accounted for in the analysis, the *right panel* shows the z band calibration error vs. redshift for an SN Ia at peak brightness (Plots are from Li et al. 2012)

are performed on cloudy nights. This transmission function is measured as a function of position on the focal plane; the rising and falling edges shift by several nanometers over the focal plane, and using this information is critical to achieve sub-percent calibration.

The second new system is an atmospheric telescope, called "AtmCam," which measures changes in the atmosphere transmission (Li et al. 2012; Stubbs et al. 2007). The motivation for AtmCam is illustrated in Fig. 4: it is primarily to measure the effect of changes in precipitable water vapor (PWV), which can affect the z band calibration at the level of $\sim$0.01 mag.

The Large Synoptic Survey Telescope (LSST Science Collaboration et al. 2009, LSST) is currently under construction and will be a significantly more powerful instrument than its predecessors. It will have an 8 m mirror ($\times$4 more area than

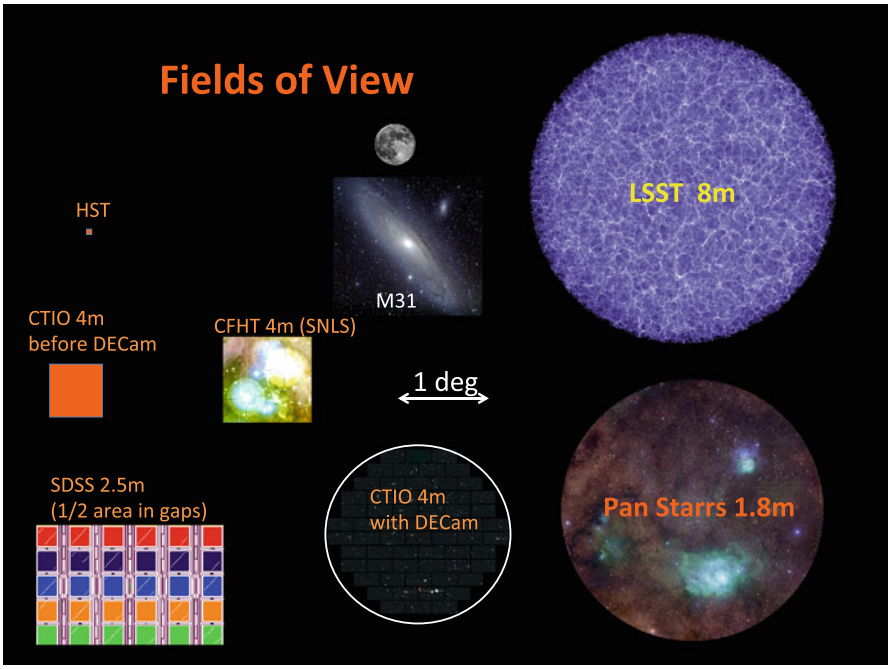

Fig. 5 For each labeled instrument, the size of the square or circle illustrates the field of view, or sky area, covered by a single telescope exposure. The moon, M31 galaxy, and a 1 degree *arrow* are shown for scale. The telescope mirror size (in meters) is indicated for each instrument

DES) nearly 10 $\deg^2$ field of view ($\times 3$ larger than DES) and advanced calibration systems to measure efficiency variations in the telescope and atmosphere. Current expectations are that tens of thousands of high-quality SN Ia light curves will be measured in the $ugrizY$ bands. Numerous independent Hubble diagrams can be made with different systematic selections such as host-galaxy properties, SN Ia color, classification probability, etc. Comparing so many high-statistics Hubble diagrams will provide unique and critical information about systematic uncertainties.

To illustrate the improving sky coverage of large surveys, Fig. 5 shows the field of view (FoV) for past, current, and future surveys. The LSST era will be spectacular, as it has a significant increase in both the FoV and the mirror size. An additional improvement, not shown in the figure, is the improved near-IR sensitivity.

5 Big Data Issues

Large SN Ia data samples bring many new challenges, some of which were described in previous sections. Here we discuss three major challenges in more detail: (1) calibration, (2) selection and fitting biases, and (3) photometric classification.

5.1 Calibration

Since calibration is currently the largest source of systematic uncertainty for the SN Ia Hubble diagram, improving the calibration is essential for improving measurements of cosmological parameters with SNe Ia. This section is far too short to give a proper treatment, so we recommend an excellent paper by Regnault et al. (2009) for those ready to dive into the details. Here we give a brief introductory overview of the calibration issues.

In many branches of science, the physical units of measurement (e.g., electron Volt, kilogram, meter) are so well calibrated that we can easily forget the underlying physical property for which these units are based. For example, if you want to measure gravitational acceleration using $g = d/t^2$ (distance divided by time squared), the precision is most likely determined by your budget to acquire accurate devices to measure distance and time. It is highly unlikely that you would ever need to know how units of distance and time are defined: how far light travels in a short time interval and radiation frequency from cesium 133. In contrast to these extremely well-defined units, astronomical magnitudes are based on comparing to a bright star, known as a "primary standard," whose absolute brightness may not be known with the desired precision. This means that SN Ia flux measurements can be measured with better (sub-percent) precision than the primary standard. So while astronomical analyses never need to examine how the meter or second is defined, defining the brightness of a primary standard is always under scrutiny.

Recall that the essential goal is to compare SN magnitudes at low and high redshift. For example, at $z = 0.05$, the rest-frame 4400 Å flux is observed in the g band, while at $z = 0.50$ this same flux is observed in the r band. Thus, comparing fluxes at these two redshifts requires a precise knowledge of the g and r band efficiencies: this is calibration. More generally, for a given rest-frame flux, the observed flux is measured in different filter bands at different redshifts, and the efficiency of each filter passband must be accurately measured. Note that calibration compares fluxes in different bands on the same telescope or from different telescopes. For example, SDSS, SNLS, and PS1 all have SDSS-like $griz$ filters. However, the transmission is slightly different on each telescope, and therefore measured transmissions are needed to correct one set of observations to accurately compare with another. Since the $griz$ filter transmissions are quite similar on each telescope (SDSS,SNLS,PS1), there is a relatively small uncertainty in comparing magnitudes among these telescopes. However, the low-z SN Ia sample was measured mostly with Bessell-like $UBVRI$ filters which are quite different than $griz$; accurately calibrating the $UBVRI$ and $griz$ filter systems at the percent level has been a major challenge.

Ideally, the telescope+atmosphere efficiency vs. wavelength would be measured well enough for sub-percent calibration, but previous surveys have not been able to do this. They have therefore relied on a relative calibration with respect to a primary *spectrophotometric* standard for which an accurate spectrum is known: Vega or BD +17 as measured by the Hubble Space Telescope (HST). SN fluxes are first compared to nearby "tertiary" stars as illustrated in Fig. 6. Ideally the same

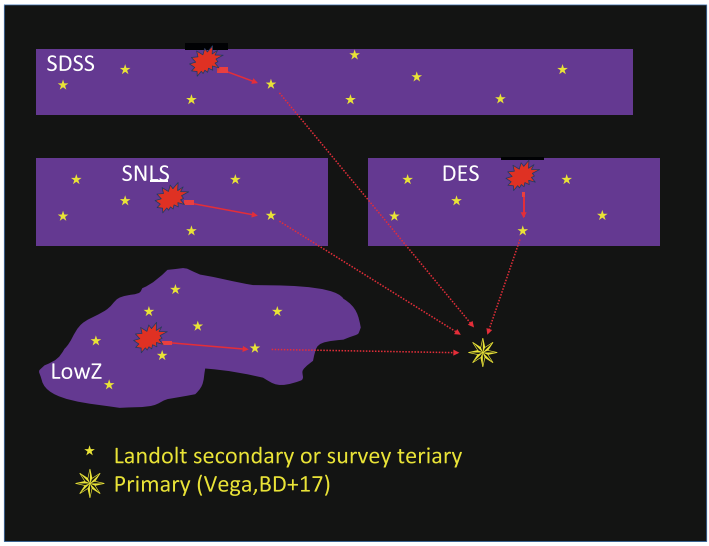

Fig. 6 Illustration of calibration between SNe observed in different fields. The *red symbols* represent the SN, and the *arrows* represent the calibration paths

survey instrument would be used to observe the HST standard, but this is difficult without saturating the CCDs. Vega is hopelessly bright for large telescopes, but BD + 17 (mag ∼10) has been observed with very short (∼1 s) exposures. Bohlin and Landolt (2015), however, have recently shown that the BD + 17 mag has been slowly changing at the level of 0.01 mag per year, and thus it is likely part of a binary system. Current projects are looking for more stable spectrophotometric standards measured with the Hubble Space Telescope (HST).

While more recent surveys use BD + 17 which can be directly observed with short exposures, Vega-based observations are more common, particular for older SN surveys. A Vega calibration relies on a network of well-measured secondary stars known as "Landolt standards" (Landolt and Umoto 2007) and also on Landolt's measurements of Vega mags. This Landolt technique was used for many of the low-z SNe Ia[1] and leads to calibration difficulties because the filter transmissions for the Landolt observations are not well known. These $UBVRI$ transmissions are approximately like those in Bessell (1990), and there has been significant effort in determining "effective Landolt filters transmissions" as well as the associated uncertainty.

In addition to stellar references and filter transmissions, uniformity is another major issue. Ideally, 1000 photons hitting a CCD pixel will give the same signal

[1]Most of the low-z SNe Ia used in cosmology analyses are from the Center for Astrophysics (Hicken et al. 2009, CfA), Carnegie Supernova Project (Contreras et al. 2010, CSP), and Lick Observatory Supernova Search (Ganeshalingam et al. 2013, LOSS).

(number of electrons) regardless of where the pixel is located. In practice, however, each pixel has a different response and must be corrected. In principle, illumination flats correct each pixel to yield a uniform response. This works well on small scales (few pixels), but is not accurate over large scales because the flat illumination is not sufficiently uniform. The standard uniformity method is to observe stars in dense stellar fields and to make many dithered observations so that a given star is observed at many different locations on the focal plane.

Flats and stellar field observations can be used to correct CCD response variations over the focal plane, but there is another uniformity challenge for scales much larger than the telescope field of view. SN surveys typically observe several different telescope pointings, some of which are separated by tens of degrees and thus have no overlap. With no common stars to observed in well-separated pointings, the challenge here is to determine a uniform zero point in each pointing. The standard technique is to interleave observations of the SN fields with observations of secondary (e.g., Landolt) or primary standards.

In previous surveys the filter transmissions were rarely measured or not measured at all. Even if the transmissions are measured before a survey begins, aging effects can cause significant and unknown changes over time. There are two specific examples to illustrate this problem. First, Doi et al. (2010) remeasured the SDSS filter transmissions and found a significant change in the u band. The second case is when the SNLS i band filter was dropped in 2008 and then replaced. To track potential time-dependent changes in the telescope transmissions, newer surveys (see DES and LSST in Sect. 4) are employing on-site calibration systems which repeatedly measure telescope transmissions throughout the survey. In addition, atmospheric monitoring has also been added since atmospheric changes can be significantly larger and more frequent than those from the telescope.

5.2 Bias Corrections

SN Ia samples are effected by selection biases, primarily from Malmquist bias in which brighter SNe are preferentially selected. Additional biases can be introduced from light curve training and fitting (Sect. 2), fitting the Hubble diagram for cosmological parameters and from core collapse (CC) contamination in a photometrically classified sample (Sect. 5.3). The impact of these biases can be evaluated with a Monte Carlo simulation (MC) of SNe Ia, which is analyzed in exactly the same manner as the data. The basic philosophy of the MC is as follows. First, a light curve model is used to randomly select a set of SN Ia properties: stretch, color, and time of explosion or peak brightness. Next, a volumetric rate model is used to select a random redshift, and a cosmology model is used to determine the distance modulus to dim the apparent brightness of the SN. The MC uses the SN properties and distance modulus to predict the flux and uncertainty that would be measured at each survey observation date (epoch). The measured zero point at each epoch is used to convert the SN magnitude into a CCD flux. The measured sky noise and point spread function (PSF) are used to predict the flux uncertainty. In short, the

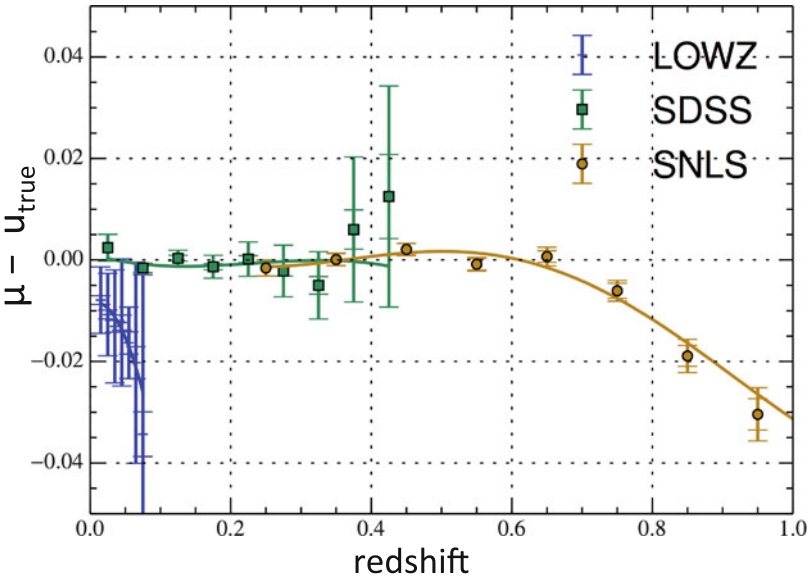

Fig. 7 For the SDSS + SNLS joint analysis (Betoule et al. 2014), MC prediction for distance-modulus bias ($\mu - \mu_{\text{true}}$) vs. redshift

survey information is used to accurately predict what the telescope would observe for a set of randomly generated SNe Ia.

To simulate CC SNe, there are no empirical stretch and color relations as with SNe Ia. Instead, well-measured CC light curves are used to create a set of interpolated templates, and a peak luminosity function is assumed, such as from Li et al. (2011). K-corrections are applied to predict the broadband magnitudes at arbitrary redshift. More details of CC simulations are in Kessler et al. (2010) and Bernstein et al. (2012).

The MC is commonly used to predict and correct the Hubble diagram bias as shown in Fig. 7 for the joint SDSS + SNLS analysis. Checking the validity of the MC is tricky and involves examining data/MC comparisons of many distributions such as the fitted light curve parameters and quantities sensitive to signal to noise. The critical MC cross-check is to compare the fitted color vs. redshift as shown in Fig. 8 for several SN Ia samples that have been used in recent cosmology analyses. The average color decreases at higher redshifts where surveys preferentially select brighter events that tend to be bluer.

The low-z sample is different because it is not from a rolling search and is instead based on follow-up observations of SNe discovered by other SN search programs. While the follow-up observations provide the zero point, sky noise, and PSF needed to perform a simulation, this information is not available for the low-z SN searches, and therefore the selection bias cannot be simulated from first principles. Although the exact low-z SN search cannot be simulated, two extreme cases can be simulated.

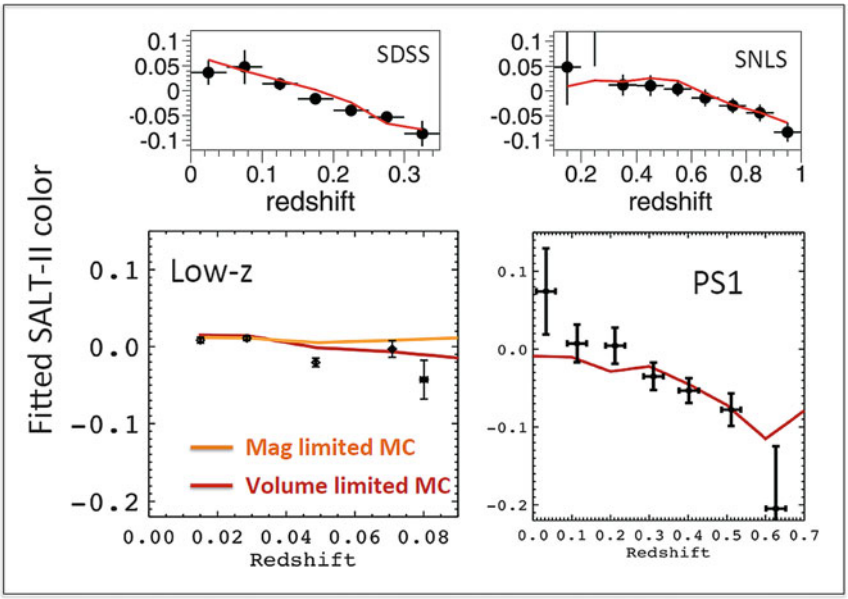

Fig. 8 Fitted SALT-II color average vs. redshift for SN Ia samples used in recent cosmology analyses. *Solid black circles* are the data, and the *lines* are MC predictions using SNANA (Kessler et al. 2009b). The two MC predictions for the low-z sample are described in the text. SDSS and SNLS plots are from their joint analysis; low-z and PS1 plots are from Scolnic et al. (2014)

The first case is a volume-limited search that is naively expected because low-z searches are largely based on targeting known galaxies. The redshift dependence on the average color and stretch is assumed to be real physical properties of SN Ia, and the search instrument is assumed to have sufficient depth to find all low-z SNe. The second case is a magnitude-limited survey as suggested by the observed trend of decreasing color with redshift. In this case, an artificial telescope is tuned so that Malmquist bias causes the redshift dependence of color and stretch. Each MC simulation has been used to predict the low-z bias (low-z panel in Fig. 8), and the difference between these two low-z bias estimates is included in the systematic uncertainty budget (Betoule et al. 2014; Scolnic et al. 2014). The resulting bias uncertainty is $\sim$0.01 mag for the low-z sample.

5.3 Photometric Classification

While previous SN Ia cosmology results were based on spectroscopically confirmed samples, increasingly large imaging surveys will find many more SNe Ia than spectroscopic resources can confirm. To take advantage of these large samples in the future (PS1, DES, LSST), we are entering a new era in which high-statistics

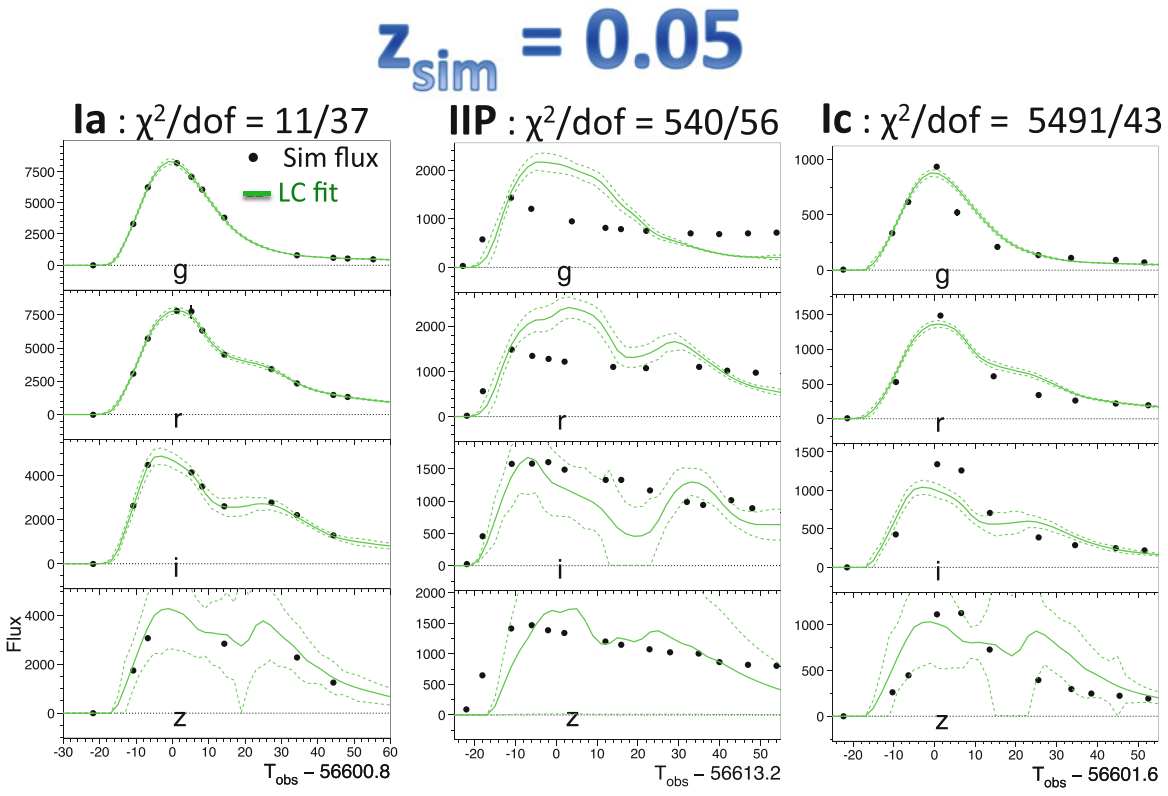

Fig. 9 For a DES-SN simulation, `SALT-II` *griz* light curve fits are shown for SNe of Type Ia (*left*), Type IIP (*middle*), and Type Ic (*right*). In the *top panels*, the generated redshift is $z = 0.05$, and the z band fit-model uncertainty is large because this wavelength range is well outside the valid range of the `SALT-II` model. In the *bottom panels*, the same SNe are generated at $z = 0.40$. Above each light curve, the best-fit chi-squared per degree of freedom is shown. The SN Ia

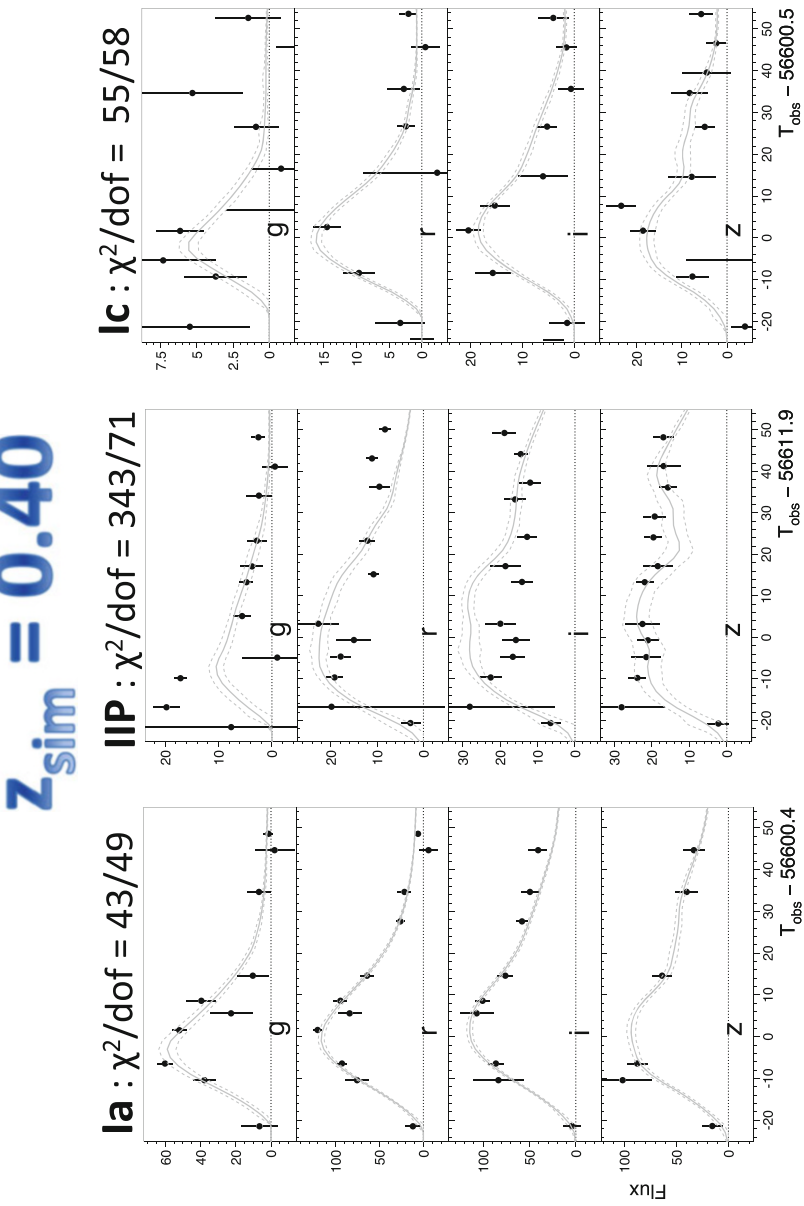

Fig. 9 (*continued*) fit is good at both redshifts. The SN IIP fit is bad at both redshifts. The SN Ic fit is bad at low redshift and good at $z = 0.40$, illustrating a potential source of contamination in a photometrically classified samplex

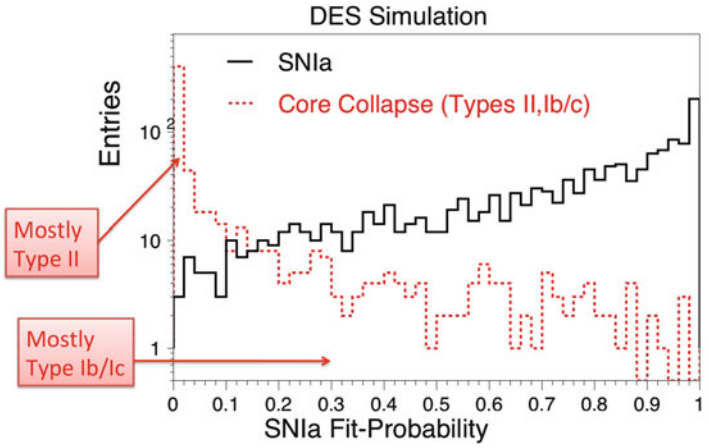

Fig. 10 For simulated SNe in the Dark Energy Survey, the `SALT-II` *light curve* fit probability distribution is shown for SNe Ia (*solid black histogram*) and for SNe CC (*dashed red*)

SN Ia Hubble diagrams will rely on "*photometric classification*" to identify SNe Ia using light curves without spectra.

The first challenge is to reject contamination from the much more numerous CC SNe. About 70 % of CC SNe are Type II; these are relatively easy to distinguish from SNe Ia because Type II SNe are much dimmer, and their relatively flat light curve shape is quite different. Type Ib/c and a small fraction of Type II, however, can be photometrically similar to SNe Ia and are considered to be the most serious contamination. Figures 9 and 10 illustrate the CC contamination for a DES-SN simulation that includes SNe Ia based on the `SALT-II` model and CC SNe as described in Sect. 5.2 and in Kessler et al. (2010) and Bernstein et al. (2012). All simulated SNe are fit with the `SALT-II` light curve model. Fig. 9 shows a light curve fit for a typical SN type Ia, II, and Ic; the SN II fit is poor at both redshifts, but the SN Ic fit has a good χ^2 at the higher redshift and can thus contribute to the contamination. For a larger simulation that samples the SN CC luminosity function, a fit probability ($P_{\rm fit}$: see Fig. 10) for each light curve is computed from the fit-χ^2 and the number of degrees of freedom. Most of the Type II light curves are much broader (and fainter) and those from SNe Ia, and thus $P_{\rm fit} \simeq 0$ resulting in easy rejection. The $P_{\rm fit}$ distribution for Type Ib/c, and a small fraction of Type II, overlaps the SN Ia $P_{\rm fit}$ distribution and results in contamination at the few percent level. Continued efforts on photometric classification will hopefully reduce the CC contamination well below these initial estimates.

A promising classification methodology is "machine-learning," which includes techniques such as nearest neighbors, random forests, and neural networks. The caveat, however, is that these methods rely on a training sample. While the spectroscopically confirmed SN Ia training sample is plentiful, there are many fewer confirmed CC SNe with well-measured light curves.

In addition to contamination, another challenge with photometric classification is to correctly identify the host galaxy (Gupta et al. 2016). While there are not enough spectroscopic resources to classify every SN, multi-fiber spectrographs can be used to measure accurate spectroscopic redshifts for most of the SN host galaxies, provided that the correct host galaxy is identified.

6 Conclusions

Using SNe Ia to precisely measure cosmological parameters is one of the most challenging experimental endeavors. It requires a dedicated team working over many years to collect data and to understand the instrumental performance in exquisite detail in order to distinguish astrophysical effects from instrumental effects. SN Ia cosmology has reached a level where results are systematics limited, so the brute-force method of building bigger telescopes with longer observing programs will not be sufficient to significantly improve cosmological constraints. More data must be accompanied by a reduction in systematic uncertainties. The good news is that the need to reduce systematic uncertainties is well recognized, and it has driven the design of large new surveys (e.g., DES, LSST), particularly in the development of new calibration equipment and techniques.

Finally, I wish to thank a few of my younger colleagues for carefully reading this article and providing useful feedback: Dan Scolnic, Rachel Cane, and James Lasker.

7 Cross-References

- ▸ Characterizing Dark Energy Through Supernovae
- ▸ Confirming Cosmic Acceleration in the Decade That Followed from SNe Ia at $z > 1$
- ▸ Discovery of Cosmic Acceleration
- ▸ History of Supernovae as Distance Indicators
- ▸ Low-z Type Ia Supernova Calibration
- ▸ The Hubble Constant from Supernovae
- ▸ The Infrared Hubble Diagram of Type Ia Supernovae
- ▸ The Peak Luminosity-Decline Rate Relationship for Type Ia Supernovae

References

Astier P, Guy J, Regnault N, Pain R, Aubourg E, Balam D, Basa S, Carlberg RG, Fabbro S, Fouchez D, Hook IM, Howell DA, Lafoux H, Neill JD, Palanque-Delabrouille N, Perrett K, Pritchet CJ, Rich J, Sullivan M, Taillet R, Aldering G, Antilogus P, Arsenijevic V, Balland C, Baumont S, Bronder J, Courtois H, Ellis RS, Filiol M, Gonçalves AC, Goobar A, Guide D, Hardin D, Lusset V, Lidman C, McMahon R, Mouchet M, Mourao A, Perlmutter S, Ripoche P, Tao C, Walton N (2006) The supernova legacy survey: measurement of Ω_M, Ω_Λ, and w from the first year data set. Astron Astrophys 447:31–48

Bernstein JP, Kessler R, Kuhlmann S, Biswas R, Kovacs E, Aldering G, Crane I, D'Andrea CB, Finley DA, Frieman JA, Hufford T, Jarvis MJ, Kim AG, Marriner J, Mukherjee P, Nichol RC, Nugent P, Parkinson D, Reis RRR, Sako M, Spinka H, Sullivan M (2012) Supernova simulations and strategies for the dark energy survey. Astrophys J 753:152

Bessell MS (1990) UBVRI passbands. PASP 102:1181–1199

Betoule M, Marriner J, Regnault N, Cuillandre JC, Astier P, Guy J, Balland C, El Hage P, Hardin D, Kessler R, Le Guillou L, Mosher J, Pain R, Rocci PF, Sako M, Schahmaneche K (2013) Improved photometrci calibration of the SNLS and SDSS SN surveys. Astron Astrophys 552:124

Betoule M, Kessler R, Guy J, Mosher J, Hardin D, Biswas R, Astier P, El-Hage P, Konig M, Kuhlmann S, Marriner J, Pain R, Regnault N, Balland C, Bassett BA, Brown PJ, Campbell H, Carlberg RG, Cellier-Holzem F, Cinabro D, Conley A, D'Andrea CB, DePoy DL, Doi M, Ellis RS, Fabbro S, Filippenko AV, Foley RJ, Frieman JA, Fouchez D, Galbany L, Goobar A, Gupta RR, Hill GJ, Hlozek R, Hogan CJ, Hook IM, Howell DA, Jha SW, Le Guillou L, Leloudas G, Lidman C, Marshall JL, Möller A, Mourão AM, Neveu J, Nichol R, Olmstead MD, Palanque-Delabrouille N, Perlmutter S, Prieto JL, Pritchet CJ, Richmond M, Riess AG, Ruhlmann-Kleider V, Sako M, Schahmaneche K, Schneider DP, Smith M, Sollerman J, Sullivan M, Walton NA, Wheeler CJ (2014) Improved cosmological constraints from a joint analysis of the SDSS-II and SNLS SN samples. Astron Astrophys 568:22

Bohlin RC, Landolt AU (2015) The CALSPEC stars P177D and P330E. Astronon J 149:122

Conley A, Guy J, Sullivan M, Regnault N, Astier P, Balland C, Basa S, Carlberg RG, Fouchez D, Hardin D, Hook IM, Howell DA, Pain R, Palanque-Delabrouille N, Perrett KM, Pritchet CJ, Rich J, Ruhlmann-Kleider V, Balam D, Baumont S, Ellis RS, Fabbro S, Fakhouri HK, Fourmanoit N, González-Gaitán S, Graham ML, Hudson MJ, Hsiao E, Kronborg T, Lidman C, Mourao AM, Neill JD, Perlmutter S, Ripoche P, Suzuki N, Walker ES (2011) Supernova constraints and systematic uncertainties from the first three years of the supernova legacy survey. Astrophys J Suppl 192:1

Contreras C, Hamuy M, Phillips MM, Folatelli G, Suntzeff NB, Persson SE, Stritzinger M, Boldt L, González S, Krzeminski W, Morrell N, Roth M, Salgado F, José Maureira M, Burns CR, Freedman WL, Madore BF, Murphy D, Wyatt P, Li W, Filippenko AV (2010) The carnegie supernova project: first photometry data release of low-redshift type Ia supernovae. Astronon J 139:519–539. doi:10.1088/0004-6256/139/2/519

Doi M, Tanaka M, Fukugita M, Gunn JE, Yasuda N, Ivezić Ž, Brinkmann J, de Haars E, Kleinman SJ, Krzesinski J, French Leger R (2010) Photometric response functions of the sloan digital sky survey imager. Astronon J 139:1628–1648

Eisenstein DJ, Zehavi I, Hogg DW, Scoccimarro R, Blanton MR, Nichol RC, Scranton R, Seo HJ, Tegmark M, Zheng Z, Anderson SF, Annis J, Bahcall N, Brinkmann J, Burles S, Castander FJ, Connolly A, Csabai I, Doi M, Fukugita M, Frieman JA, Glazebrook K, Gunn JE, Hendry JS, Hennessy G, Ivezić Z, Kent S, Knapp GR, Lin H, Loh YS, Lupton RH, Margon B, McKay TA, Meiksin A, Munn JA, Pope A, Richmond MW, Schlegel D, Schneider DP, Shimasaku K, Stoughton C, Strauss MA, SubbaRao M, Szalay AS, Szapudi I, Tucker DL, Yanny B, York DG (2005) Detection of the baryon acoustic peak in the large-scale correlation function of SDSS luminous red galaxies. Astrophys J 633:560–574

Flaugher B, Diehl HT, Honscheid K, Abbott TMC, Alvarez O, Angstadt R, Annis JT, Antonik M, Ballester O, Beaufore L, Bernstein GM, Bernstein RA, Bigelow B, Bonati M, Boprie D, Brooks D, Buckley-Geer EJ, Campa J, Cardiel-Sas L, Castander FJ, Castilla J, Cease H, Cela-Ruiz JM, Chappa S, Chi E, Cooper C, da Costa LN, Dede E, Derylo G, DePoy LD, de Vicente J, Doel P, Drlica-Wagner A, Eiting J, Elliott AE, Emes J, Estrada J, Fausti Neto A, Finley DA, Flores R, Frieman J, Gerdes D, Gladders MD, Gregory B, Gutierrez GR, Hao J, Holland SE, Holm S, Huffman D, Jackson C, James DJ, Jonas M, Karcher A, Karliner I, Kent S, Kessler R, Kozlovsky M, Kron RG, Kubik D, Kuehn K, Kuhlmann S, Kuk K, Lahav O, Lathrop A, Lee J, Levi ME, Lewis P, Li TS, Mandrichenko I, Marshall JL, Martinez G, Merritt KW, Miquel R, Muñoz F, Neilsen EH, Nichol RC, Nord B, Ogando R, Olsen J, Palaio N, Patton K, Peoples J, Plazas AA, Rauch J, Reil K, Rheault JP, Roe NA, Rogers H, Roodman A, Sanchez E, Scarpine

V, Schindler RH, Schmidt R, Schmitt R, Schubnell M, Schultz K, Schurter P, Scott L, Serrano S, Shaw TM, Smith RC, Soares-Santos M, Stefanik A, Stuermer W, Suchyta E, Sypniewski A, Tarle G, Thaler J, Tighe R, Tran C, Tucker D, Walker AR, Wang G, Watson M, Weaverdyck C, Wester W, Woods R, Yanny B (2015) The DES collaboration, the dark energy camera. Astronon J 150:150

Frieman JA, Bassett B, Becker A, Choi C, Cinabro D, DeJongh F, Depoy DL, Dilday B, Doi M, Garnavich PM, Hogan CJ, Holtzman J, Im M, Jha S, Kessler R, Konishi K, Lampeitl H, Marriner J, Marshall JL, McGinnis D, Miknaitis G, Nichol RC, Prieto JL, Riess AG, Richmond MW, Romani R, Sako M, Schneider DP, Smith M, Takanashi N, Tokita K, van der Heyden K, Yasuda N, Zheng C, Adelman-McCarthy J, Annis J, Assef RJ, Barentine J, Bender R, Blandford RD, Boroski WN, Bremer M, Brewington H, Collins CA, Crotts A, Dembicky J, Eastman J, Edge A, Edmondson E, Elson E, Eyler ME, Filippenko AV, Foley RJ, Frank S, Goobar A, Gueth T, Gunn JE, Harvanek M, Hopp U, Ihara Y, Ivezić Ž, Kahn S, Kaplan J, Kent S, Ketzeback W, Kleinman SJ, Kollatschny W, Kron RG, Krzesiński J, Lamenti D, Leloudas G, Lin H, Long DC, Lucey J, Lupton RH, Malanushenko E, Malanushenko V, McMillan RJ, Mendez J, Morgan CW, Morokuma T, Nitta A, Ostman L, Pan K, Rockosi CM, Romer AK, Ruiz-Lapuente P, Saurage G, Schlesinger K, Snedden SA, Sollerman J, Stoughton C, Stritzinger M, Subba Rao M, Tucker D, Vaisanen P, Watson LC, Watters S, Wheeler JC, Yanny B, York D (2008) The sloan digital sky survey-II supernova survey: technical summary. Astronon J 135:338–347

Ganeshalingam M, Li W, Filippenko AV (2013) Constraints on dark energy with the LOSS SN Ia sample. MNRAS 433:2240–2258. doi:10.1093/mnras/stt893

Gupta RR, Kuhlmann S, Kovacs E, Spinka H, Kessler R, Goldstein DA, Liotine C, Pomian K, D'Andrea CB, Sullivan M, Carretero J, Castander FJ, Nichol RC, Finley DA, Fischer JA, Foley RJ, Kim AG, Papadopoulos A, Sako M, Scolnic DM, Smith M, Tucker BE, Uddin S, Wolf RC, Yuan F, Abbott TMC, Abdalla FB, Benoit-Levy A, Bertin E, Brooks D, Carnero Rosell A, Carrasco Kind M, Cunha CE, da Costa LN, Desai S, Doel P, Eifler TF, Evrard AE, Flaugher B, Fosalba P, Gaztanaga E, Gruen D, Gruendl R, James DJ, Kuehn K, Kuropatkin N, Maia MAG, Marshall JL, Miquel R, Plazas AA, Romer AK, Sanchez E, Schubnell M, Sevilla-Noarbe I, Sobreira F, Suchyta E, Swanson MEC, Tarle G, Walker AR, Wester W (2016) Host galaxy identification for supernova surveys. ArXiv e-prints

Guy J, Sullivan M, Conley A, Regnault N, Astier P, Balland C, Basa S, Carlberg RG, Fouchez D, Hardin D, Hook IM, Howell DA, Pain R, Palanque-Delabrouille N, Perrett KM, Pritchet CJ, Rich J, Ruhlmann-Kleider V, Balam D, Baumont S, Ellis RS, Fabbro S, Fakhouri HK, Fourmanoit N, González-Gaitán S, Graham ML, Hsiao E, Kronborg T, Lidman C, Mourao AM, Perlmutter S, Ripoche P, Suzuki N, Walker ES (2010) The supernova legacy survey 3-year sample: type Ia SN photometric distances and cosmological constraints. Astron Astrophys 523:7

Hicken M, Wood-Vasey WM, Blondin S, Challis P, Jha S, Kelly PL, Rest A, Kirshner RP (2009) Improved dark energy constraints from ˜100 new CfA supernova type Ia light curves. Astrophys J 700:1097–1140. doi:10.1088/0004-637X/700/2/1097

Kaiser N, Aussel H, Burke BE, Boesgaard H, Chambers K, Chun MR, Heasley JN, Hodapp KW, Hunt B, Jedicke R, Jewitt D, Kudritzki R, Luppino GA, Maberry M, Magnier E, Monet DG, Onaka PM, Pickles AJ, Rhoads HHP, Simon T, Szalay A, Szapudi I, Tholen DJ, Tonry JL, Waterson M, Wick J 2002 Pan-STARRS: a large synoptic survey telescope array, In: Tyson JA, Wolff S (eds) survey and other telescope technologies and discoveries, vol 4836. Society of Photo-optical Instrumentation Engineers, Bellingham, pp 154–164. doi:10.1117/12.457365

Kessler R, Becker AC, Cinabro D, Vanderplas J, Frieman JA, Marriner J, Davis TM, Dilday B, Holtzman J, Jha SW, Lampeitl H, Sako M, Smith M, Zheng C, Nichol RC, Bassett B, Bender R, Depoy DL, Doi M, Elson E, Filippenko AV, Foley RJ, Garnavich PM, Hopp U, Ihara Y, Ketzeback W, Kollatschny W, Konishi K, Marshall JL, McMillan RJ, Miknaitis G, Morokuma T, Mörtsell E, Pan K, Prieto JL, Richmond MW, Riess AG, Romani R, Schneider DP, Sollerman J, Takanashi N, Tokita K, van der Heyden K, Wheeler JC, Yasuda N, York D (2009a) First-Year sloan digital sky survey-II supernova results: hubble diagram and cosmological parameters. Astrophys J Suppl 185:32–84

Kessler R, Bernstein JP, Cinabro D, Dilday B, Frieman JA, Jha S, Kuhlmann S, Miknaitis G, Sako M, Taylor M, Vanderplas J (2009b) SNANA: a public software package for supernova analysis. PASP 121:1028–1035

Kessler R, Bassett B, Belov P, Bhatnagar V, Campbell H, Conley A, Frieman JA, Glazov A, González-Gaitán S, Hlozek R, Jha S, Kuhlmann S, Kunz M, Lampeitl H, Mahabal A, Newling J, Nichol RC, Parkinson D, Philip NS, Poznanski D, Richards JW, Rodney SA, Sako M, Schneider DP, Smith M, Stritzinger M, Varughese M (2010) Results from the supernova photometric classification challenge. PASP 122:1415–1431

Landolt A, Umoto A (2007) Optical multicolor photometry of spectrophotometric standard stars. Astron J 133:768

Li T, DePoy DL, Kessler R, Burke DL, Marshall JL, Wise J, Rheault JP, Carona DW, Boada S, Prochaska T, Allen R (2012) aTmcam: a simple atmospheric transmission monitoring camera for sub 1 % photometric precision. In: Society of photo-optical instrumentation engineers (SPIE) conference series. Society of Photo-Optical Instrumentation Engineers (SPIE) conference series, vol 8446, p 2

Li W, Leaman J, Chornock R, Filippenko AV, Poznanski D, Ganeshalingam M, Wang X, Modjaz M, Jha S, Foley RJ, Smith N (2011) Nearby supernova rates from the lick observatory supernova search – II. The observed luminosity functions and fractions of supernovae in a complete sample. MNRAS 412:1441–1472

LSST Science Collaboration, Abell PA, Allison J, Anderson SF, Andrew JR, Angel JRP, Armus L, Arnett D, Asztalos SJ, Axelrod TS, et al (2009) LSST science book, Version 2.0. arXiv:0912.0201

Mosher J, Guy J, Kessler R, Astier P, Marriner J, Betoule M, Sako M, El-Hage P, Biswas R, Pain R, Kuhlmann S, Regnault N, Frieman JA, Schneider DP (2014) Cosmological parameter uncertainties from the SALT-II type Ia SN lightcurve models. Astrophys J 793:16

Nugent P, Kim A, Perlmutter S (2002) K-Corrections and extinction corrections for type Ia supernovae. PASP 114:803–819

Perlmutter S, Aldering G, Goldhaber G, Knop RA, Nugent P, Castro PG, Deustua S, Fabbro S, Goobar A, Groom DE, Hook IM, Kim AG, Kim MY, Lee JC, Nunes NJ, Pain R, Pennypacker CR, Quimby R, Lidman C, Ellis RS, Irwin M, McMahon RG, Ruiz-Lapuente P, Walton N, Schaefer B, Boyle BJ, Filippenko AV, Matheson T, Fruchter AS, Panagia N, Newberg HJM, Couch WJ, Project TSC (1999) Measurements of omega and lambda from 42 high-redshift supernovae. Astrophys J 517 565–586. doi:10.1086/307221

Perrett K, Balam D, Sullivan M, Pritchet C, Conley A, Carlberg R, Astier P, Balland C, Basa S, Fouchez D, Guy J, Hardin D, Hook IM, Howell DA, Pain R, Regnault N (2010) Real-time analysis and selection biases in the supernova legacy survey. Astron J 140:518–532

Regnault N, Conley A, Guy J, Sullivan M, Cuillandre JC, Astier P, Balland C, Basa S, Carlberg RG, Fouchez D, Hardin D, Hook IM, Howell DA, Pain R, Perrett K, Pritchet CJ (2009) Photometric calibration of the supernova legacy survey Fields. Astron Astrophys 506:999–1042

Riess AG, Filippenko AV, Challis P, Clocchiatti A, Diercks A, Garnavich PM, Gilliland RL, Hogan CJ, x Jha AV, Kirshner RP, Leibundgut B, Phillips MM, Reiss D, Schmidt BP, Schommer RA, Smith RC, Spyromilio J, Stubbs C, Suntzeff NB, Tonry J (1998) Observational evidence from SN for an accelerating universe and a cosmological constant. Astron J 116:1009–1038

Schlafly EF, Finkbeiner DP, Jurić M, Magnier EA, Burgett WS, Chambers KC, Grav T, Hodapp KW, Kaiser N, Kudritzki RP, Martin NF, Morgan JS, Price PA, Rix HW, Stubbs CW, Tonry JL, Wainscoat RJ (2012) Photometric calibration of the first 1.5 years of the pan-STARRS1 survey. Astrophys J 756:158

Scolnic D, Rest A, Riess A, Huber ME, Foley RJ, Brout D, Chornock R, Narayan G, Tonry JL, Berger E, Soderberg AM, Stubbs CW, Kirshner RP, Rodney S, Smartt SJ, Schlafly E, Botticella MT, Challis P, Czekala I, Drout M, Hudson MJ, Kotak R, Leibler C, Lunnan R, Marion GH, McCrum M, Milisavljevic D, Pastorello A, Sanders NE, Smith K, Stafford E, Thilker D, Valenti S, Wood-Vasey WM, Zheng Z, Burgett WS, Chambers KC, Denneau L, Draper PW, Flewelling H, Hodapp KW, Kaiser N, Kudritzki RP, Magnier EA, Metcalfe N, Price PA, Sweeney W, Wainscoat R, Waters C (2014) Systematic uncertainties associated with

the cosmological analysis of the first pan-STARRS1 type Ia supernova sample. Astrophys J 795:45

Scolnic D, Casertano S, Riess AG, Rest A, Schlafly E, Foley RJ, Finkbeiner D, Tang C, Burgett WS, Chambers KC, Draper PW, Flewelling H, Hodapp KW, Huber ME, Kaiser N, Kudritzki RP, Magnier EA, Metcalfe N, Stubbs CW (2015) Supercal: cross-calibration of multiple photometric systems to improve cosmological measurements with type Ia supernovae. ArXiv:1508.05361 (Accepted for publication in ApJ)

Stubbs CW, High FW, George MR, DeRose KL, Blondin S, Tonry JL, Chambers KC, Granett BR, Burke DL, Smith RC (2007) Toward more precise survey photometry for panSTARRS and LSST: measuring directly the optical transmission spectrum of the atmosphere. PASP 119:1163–1178